Sombrero Uplift Above the Altiplano-Puna Magma Body: Evidence of a Ballooning Mid-Crustal Diapir

Yuri Fialko* and Jill Pearse†

The Altiplano-Puna ultralow-velocity zone in the central Andes, South America, is the largest active magma body in Earth's continental crust. Space geodetic observations reported an uplift in the Altiplano-Puna proper at a rate of ~10 mm/year; however, the nature of the inferred inflation source has been uncertain. We present data showing that the uplift has persisted at a nearly constant rate over the past two decades, and is surrounded by a broad zone of subsidence. We show that the ongoing uplift and peripheral subsidence may result from a large mid-crustal diapir fed by partial melt from the Altiplano-Puna Magma Body.

There is a long-standing debate on the mechanisms of transport of silicic melts from the source region to the final emplacement levels in the upper crust. Once-prevailing views of slow transport of silicic melts in crustal diapirs (1) have been challenged by considerations of thermal viability of diapirs and suggestions that most of granitic melts are transported to the upper crust in dikes (2, 3). Subsequent theoretical studies have shown that granitic dikes may have difficulty leaving the source region (4) and that diapirs may not in fact be in danger of freezing if one relaxes simplifying assumptions about the rheology of the ductile lower crust—for example, by explicitly considering temperature-dependent power-law creep (5).

Magma transport through the crust may be accompanied by deformation of Earth's surface. Geodetic observations in neovolcanic areas commonly reveal episodes of uplift due to inflation of magma bodies in Earth's upper crust (6–11), possibly indicating injection of dikes from deeper sources. No observations of surface deformation due to magmatic diapirs have been reported so far. Expected features of diapir-related deformation include nearly constant surface velocities, large spatial wavelengths (on the order of tens of kilometers or more), axisymmetric patterns, and association with robust magmatic activity. Here, we investigated a long-term, long-wavelength crustal uplift in the Altiplano-Puna province in South America, a site of intense silicic volcanism over the past 10 million years. The Altiplano-Puna volcanic province belongs to an active volcanic arc in the central Andes, extending through Peru, southwestern Bolivia, Chile, and northwestern Argentina (12, 13). The province hosts a number of large calderas formed as a result of catastrophic eruptions. Seismic observations revealed that much of the volcanic province is underlain by a massive ultra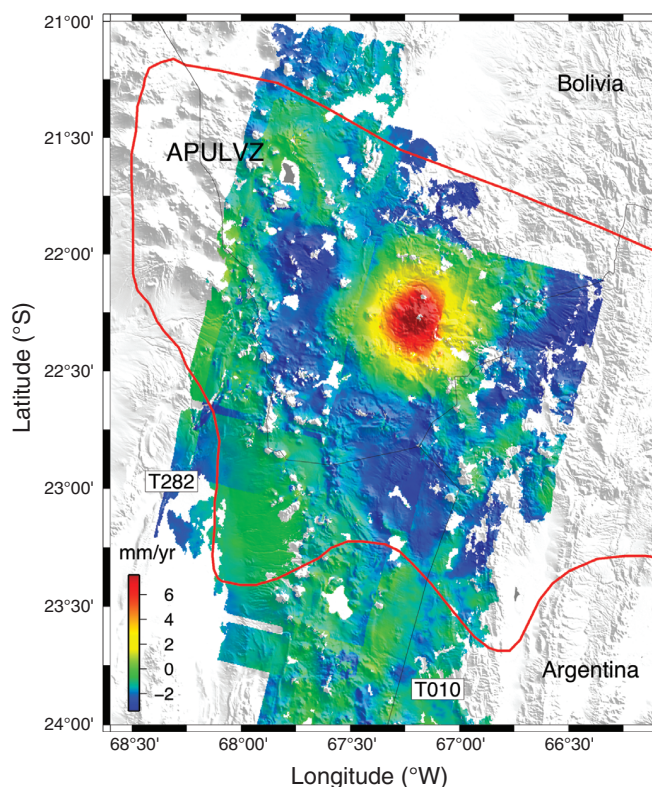low-velocity zone (ULVZ) at a depth of 17 to 19 km (14, 15). The Altiplano-Puna Ultralow-Velocity Zone (APULVZ) has thickness on the order of 1 km and lateral extent on the order of 100 km, and is believed to be the largest known active magma body in Earth's continental crust (15).

Space geodetic surveys using interferometric synthetic aperture radar (InSAR) identified surface uplift within the APULVZ proper (16). This uplift was attributed to the Uturuncu volcano, although that volcano has remained dormant over the past 2.7×10^5 years (16, 17). The surface uplift field with a spatial wavelength of tens of kilometers requires either a deep (depth >15 km) or an areally extensive (characteristic diameter >20 km) source of inflation (16). Because InSAR data from only one look direction are not sufficient to constrain the depth and geometry of pressurized magma bodies (10, 18), understanding the nature of uplift in the Altiplano-Puna province requires measurements of both the vertical and horizontal components of deformation.

To reduce uncertainties in the depth estimates of the inferred inflation source, in 2006 we asked the European Space Agency to task the ERS-2 and EnviSAT satellites to acquire data from both the ascending and descending orbits over the APULVZ. Several tens of acquisitions were made, increasing the total time span of observations from 1992 until 2010. Average line-of-sight (LOS) velocities from several satellite tracks covering APULVZ (Fig. 1) indicate that the central uplift near the Uturuncu volcano is surrounded by a broader region of subsidence at a rate that is much smaller than the peak uplift rate (19). The peripheral subsidence was not detected in previous studies, presumably because of a shorter time span of observations and a lower signal-to-noise ratio. We refer to the observed deformation pattern (Fig. 1) as the "sombrero uplift." Analysis of time dependence of surface unrest indicates that the latter has persisted over the past two decades (Fig. 2 and fig. S2). The monotonic uplift in the center of the APULVZ contrasts with episodic inflation typical of shallow magma bodies in the upper crust (7, 11, 20) but is similar to deformation associated with another large mid-crustal magma body in the Rio Grande Rift in New Mexico (21, 22).

We used the average LOS velocities from different radar look directions to constrain the depth of the inflation source (fig. S2). Joint inversions of average LOS velocities are subject to several uncertainties because of the relative nature of

Institute of Geophysics and Planetary Physics, Scripps Institution of Oceanography, University of California, San Diego, La Jolla, CA 92093, USA.

*To whom correspondence should be addressed. E-mail: yfialko@ucsd.edu
†Present address: Alberta Geological Survey, Edmonton, Alberta T6B 2X3, Canada.

Fig. 1. Mosaic of LOS velocities obtained from stacking of ERS-1/2 and EnviSAT data from the descending tracks 282 and 10. Motion toward the satellite is taken to be positive. The LOS velocity is constrained to have a zero mean value in the far field, away from the imaged deformation anomaly. Note a ring of subsidence surrounding the central uplift. Red line denotes the extent of the seismically imaged ULVZ in the middle crust (14, 15).

InSAR measurements, different time spans of acquisitions from different satellite tracks, and possible temporal variations in the uplift rate. In addition, in cases of superposition of the central uplift and peripheral subsidence (Fig. 1), inversions that consider a single source of inflation result in underestimation of the source depth.

To avoid biases due to the source complexity, we use positions of the LOS velocity maxima that are independent of the estimated uplift rates. The data from the descending (fig. S2, A and C) and ascending (fig. S2B) satellite orbits show that peaks in the LOS velocity anomalies are separated by as much as 8 ± 2 km. This separation stems from the contribution of horizontal displacements to changes in the radar range (10). Forward modeling indicates that the separation increases with the source depth for a given source geometry; for oblate (sill-like) sources, it also increases with the source diameter for a given source depth. Models assuming an oblate source geometry and elastic deformation of the host rocks (23) fail to produce the observed separation between peaks in the LOS velocities (fig. S2); the maximum predicted separation is 3 to 5 km for sills shallower than 12 km. This result implies that (i) the inflation source may be spheroidal or prolate in shape, (ii) the source is located below the brittle-ductile transition, and (iii) the assumption of purely elastic deformation is invalid.

We performed numerical experiments to evaluate the effect of stress relaxation in the middle crust on surface velocities (19). We found that the main effect of viscous deformation is to reduce

the contribution of the horizontal component of the velocity field with respect to the vertical component (fig. S4). A smaller ratio of horizontal to vertical displacements translates into a smaller separation between the maxima in the LOS displacements from the descending and ascending orbits, which lends further support to the inference of a prolate source geometry. We note that shallow (depth <15 km) isometric or prolate sources in elastic half-space can be ruled out, as they are not able to generate an uplift anomaly of sufficiently large wavelength. An upper bound on the source depth is likely provided by the seismically imaged ULVZ. This is because the massive partially molten APULVZ (14, 15) is likely to absorb strain from hypothetical underlying sources, thereby precluding a localized deformation at Earth's surface. The same argument can be invoked against a deep deflation source as a possible cause of peripheral subsidence (Fig. 1).

Although it is possible to fit the InSAR data by a simple elastic half-space model consisting of two point sources of volume change (Mogi sources; fig. S3), such a model may be deemed unreasonable on the basis of the following considerations. First, the inflating and deflating Mogi sources would have to reside at depths of at least 25 and 80 km, respectively, to explain the observed wavelength of surface deformation (Fig. 1 and fig. S3). These source depths are greater than those of the brittle-ductile transition and the APULVZ (14, 15), so that the assumption of elastic deformation is inapplicable, as discussed above. Second, the inferred rate of deflation of

the hypothesized deep source exceeds the inflation rate of the shallower source by a factor of 4 or more, raising an issue of mass balance. Third, a long-term surface uplift (Fig. 2) would imply either a permanent magma conduit with a constant flow rate connecting the upper mantle source to the mid-crustal magma body, or a quasi-steady supply of melt to the mid-crustal magma body via frequent magma-driven fractures. Mechanical and thermal considerations suggest that such scenarios are unlikely (19). Alternatively, the persistent nature of surface deformation may be attributed to slow viscous deformation induced by a large magma body in the middle crust (22).

We explored the possibility that the observed sombrero uplift is associated with the Altiplano-Puna Magma Body itself. As an initial test of this hypothesis, we ran a series of inverse models using a combination of an inflating source and a grid of deflating Mogi sources at the seismically inferred depth of the APULVZ. The grid was designed to match the extent of the observed surface subsidence (Fig. 1). An inflating source was represented by a prolate spheroid (24, 25). The depth of the inflating source deduced from these inversions was not resolvably different from the assumed depth of the distributed deflating source representing the APULVZ. Furthermore, the rate of volume change was found to be approximately equal for the inflating and deflating sources. Although this simple kinematic model is able to fit the data, it does not explain the mechanism of volume changes at depth. Note that a sill-like body with interconnected melt cannot maintain substantial lateral gradients in the magma pressure (e.g., an overpressure in the center of the body and an underpressure elsewhere).

Instead, we propose that the sombrero uplift (Fig. 1) results from ballooning of a large diapir fed by hot low-viscosity material from the APULVZ. One possibility is that partial melting in the APULVZ produces magma of lower density relative to the host rocks, which may result in the Rayleigh-Taylor instability in the roof of the magma body and formation of a buoyant diapir. As such a diapir increases in size, it may be fed by lateral migration of partial melt within the APULVZ. According to this model, inflation of the buoyant diapir causes central uplift, and withdrawal of material from the parental APULVZ is responsible for the peripheral subsidence. Note that the optimal location for the development of a diapir is in the middle of the APULVZ, consistent with seismologic and geodetic observations (Fig. 1). The inferred depth of the magma source is also consistent with available petrological constraints (17).

To test this hypothesis, we performed time-dependent 3D numerical simulations of deformation due to a buoyant diapir in the center of the APULVZ. Simulations were carried out using a finite element code, Abaqus (26). The model domain is a cylinder with a radius of 300 km and thickness of 200 km. The model includes an elastic crust with thickness of 12 km and a viscoelastic substrate. The viscoelastic substrate obeys the
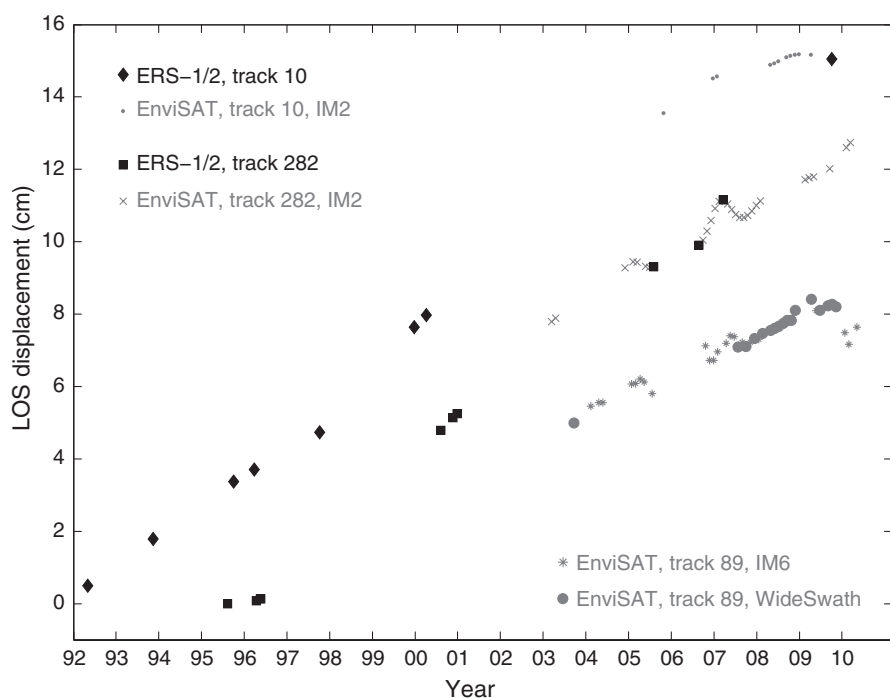
Fig. 2. Time series of LOS displacements calculated using data from the ERS (black symbols) and EnviSAT (gray symbols) acquisitions from tracks 10 (diamonds and dots), 282 (squares and crosses), and 89 (circles and asterisks). Origin of the time series is arbitrary. Locations of the reference sites are denoted by the respective symbols in fig. S2. Small-scale subannual undulations seen in LOS displacements are most likely of atmospheric origin.

temperature-dependent power-law rheology with laboratory-derived material parameters [see (*19*) for details of numerical implementation and material parameters]. The source region is approximated by a tabular body having the areal extent of the APULVZ (Fig. 1) and thickness of 1.5 km. The upper boundary of the source region is located at a depth of 19 km below the free surface. The buoyant region is approximated by a semi-ellipsoid of rotation with vertical semi-axis of 6.5 km and horizontal semi-axis of 5 km, extending 5 km above the upper boundary of the APULVZ (fig. S6). Both the diapir and the tabular source region representing the APULVZ are prescribed a linear Maxwell viscoelastic rheology. The material within the diapir has a lower density relative to the host rocks. The material within the source region is assumed to be neutrally buoyant, so that it is passively entrained by the ascending diapir. Depending on the value of melt fraction in the APULVZ, lateral transport of melt toward the central upwelling may occur as either channel or porous flow. We approximate both processes by allowing bulk viscous deformation inside the diapir and the tabular source region to ensure conservation of mass. Figure 3 shows predictions of the best-fitting "ballooning diapir" model. As can be seen in Fig. 3, the wavelength, pattern, and amplitude of predicted surface velocities are in good agreement with InSAR observations. The peak uplift velocity predicted by our best-fit model is on the order of 10 mm/year after ~20 years of deformation, and gradually decreases with time. The predicted separation between

peak LOS velocities corresponding to the ascending and descending satellite orbits is 6 km, in overall agreement with InSAR observations (fig. S2).

Our observations and modeling results therefore suggest that the ongoing sombrero uplift in the Altiplano-Puna province (Fig. 1) manifests as the formation of a large diapir in the roof of the Altiplano-Puna Magma Body. It is instructive to compare deformation due to the APULVZ to that due to the Socorro Magma Body (SMB) in central New Mexico, arguably the second largest magma body in Earth's continental crust (*27*). The two magma bodies occur in very different tectonic settings but nonetheless share a number of remarkable similarities. Both magma bodies are located in the middle crust just above a depth of 20 km. Both bodies are associated with seismic activity in the upper crust, and the long-term uplift rate is on the order of millimeters per year (*17*, *22*, *23*, *28*). In both cases, the modeled source of inflation is smaller than the seismically imaged magma body (*22*). There is indication of subsidence around the central uplift due to the SMB (*10*, *21*, *22*), although the rates of both uplift and subsidence due to the SMB are smaller than those due to the Altiplano-Puna Magma Body and therefore subject to greater uncertainties (Fig. 3). These similarities, along with modeling results presented in this study, suggest that the uplift and peripheral subsidence due to the SMB might also manifest as the formation of a magmatic diapir, rather than viscous response to inflation of a large sill-like magma body, as suggested previously (*10*, *22*). Models predict

that in both cases the surface uplift should gradually slow down and increase in wavelength, provided there is no supply of fresh melt from a deeper (e.g., mantle) source. However, the details of surface deformation (e.g., the ratio of maximum horizontal to maximum vertical displacements; fig. S4) may be sufficiently different for the sill and diapir models. The competing hypotheses therefore can be tested with further observations at the Altiplano-Puna and Socorro sites, as well as other areas of long-term uplift due to mid-crustal magma bodies. In the absence of direct observations of magma transport at depth, space geodetic surveys in neovolcanic areas can provide critical constraints on the occurrence, time scale, and dynamics of magmatic diapirism.

References and Notes

1. B. Marsh, *Am. J. Sci.* **282**, 808 (1982).
2. J. D. Clemens, C. K. Mawer, *Tectonophysics* **204**, 339 (1992).
3. N. Petford, A. R. Cruden, K. J. McCaffrey, J. L. Vigneresse, *Nature* **408**, 669 (2000).
4. A. M. Rubin, *J. Geophys. Res.* **100**, 5911 (1995).
5. R. Weinberg, Y. Podladchikov, *J. Geophys. Res.* **99**, 9543 (1994).
6. J. Langbein, D. Hill, T. Parker, S. Wilkinson, *J. Geophys. Res.* **98**, 15851 (1993).
7. J. Dvorak, D. Dzurisin, *Rev. Geophys.* **35**, 343 (1997).
8. F. Amelung, S. Jónsson, H. Zebker, P. Segall, *Nature* **407**, 993 (2000).
9. P. Lundgren et al., *J. Geophys. Res.* **106**, 19355 (2001).
10. Y. Fialko, M. Simons, Y. Khazan, *Geophys. J. Int.* **146**, 191 (2001).
11. W.-L. Chang, R. B. Smith, C. Wicks, J. M. Farrell, C. M. Puskas, *Science* **318**, 952 (2007).
12. S. L. de Silva, *Geology* **17**, 1102 (1989).
13. R. Allmendinger, T. Jordan, S. Kay, B. Isacks, *Annu. Rev. Earth Planet. Sci.* **25**, 139 (1997).
14. J. Chmielowski, G. Zandt, C. Haberland, *Geophys. Res. Lett.* **26**, 783 (1999).
15. G. Zandt, M. Leidig, J. Chmielowski, D. Baumont, X. Yuan, *Pure Appl. Geophys.* **160**, 789 (2003).
16. M. E. Pritchard, M. Simons, *Nature* **418**, 167 (2002).
17. R. S. J. Sparks et al., *Am. J. Sci.* **308**, 727 (2008).
18. J. Dieterich, R. Decker, *J. Geophys. Res.* **80**, 4094 (1975).
19. See supplementary materials on *Science* Online.
20. J. Langbein, D. Dzurisin, G. Marshall, R. Stein, J. Rundle, *J. Geophys. Res.* **100**, 12487 (1995).
21. S. Larsen, R. Reilinger, L. Brown, *J. Geophys. Res.* **91**, 6283 (1986).
22. J. Pearse, Y. Fialko, *J. Geophys. Res.* **115**, B07413 (2010).
23. Y. Fialko, Y. Khazan, M. Simons, *Geophys. J. Int.* **146**, 181 (2001).
24. X.-M. Yang, P. M. Davis, J. H. Dieterich, *J. Geophys. Res.* **93**, 4249 (1988).
25. Y. Fialko, M. Simons, *J. Geophys. Res.* **105**, 21781 (2000).
26. Abaqus/Simulia: A general purpose three-dimensional finite element program, www.3ds.com/products/simulia/overview/, v6.11 (2012).
27. J. P. Ake, A. R. Sanford, *Bull. Seismol. Soc. Am.* **78**, 1335 (1988).
28. R. E. Reilinger, J. E. Oliver, L. D. Brown, A. R. Sanford, E. I. Balazs, *Geology* **8**, 291 (1980).

Supplementary Materials
www.sciencemag.org/cgi/content/full/338/6104/250/DC1
Materials and Methods
Supplementary Text
Figs. S1 to S6
References (*29–37*)
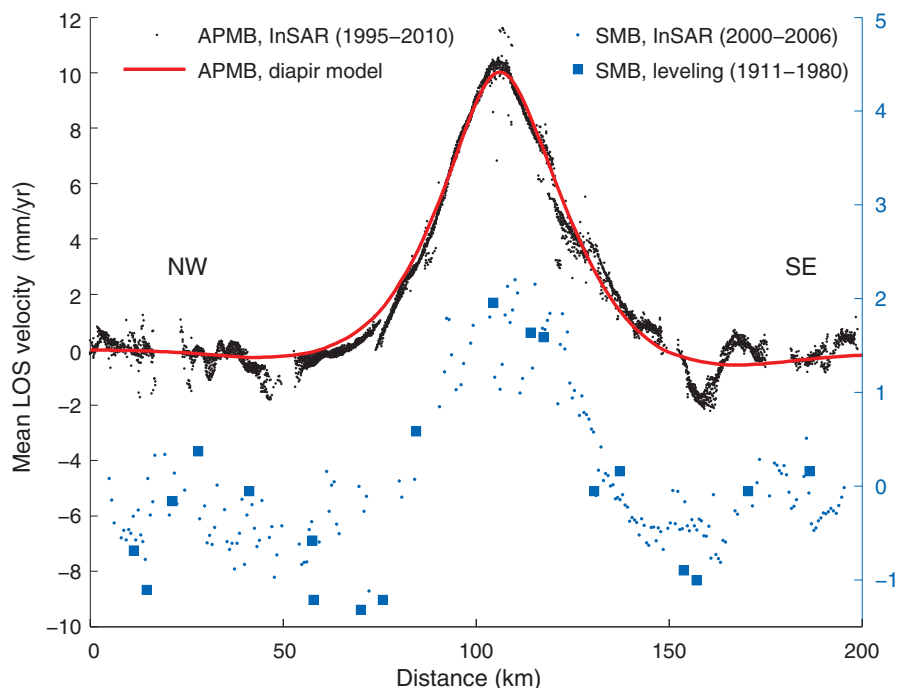
Fig. 3. Observed (black dots) and predicted (solid red line) LOS velocities along the northwest-to-southeast profile crossing the center of the uplift (Fig. 1). The model predictions correspond to a buoyant diapir at the top of the APULVZ, with density contrast of 400 kg m^{-3}. Shown at the bottom are surface velocities due to the Socorro Magma Body (New Mexico) from InSAR and leveling measurements (blue symbols, right axis).